

# We are IntechOpen, the world's leading publisher of Open Access books Built by scientists, for scientists

6,900

Open access books available

186,000

International authors and editors

200M

Downloads

Our authors are among the

154

Countries delivered to

TOP 1%

most cited scientists

12.2%

Contributors from top 500 universities



WEB OF SCIENCE™

Selection of our books indexed in the Book Citation Index  
in Web of Science™ Core Collection (BKCI)

Interested in publishing with us?  
Contact [book.department@intechopen.com](mailto:book.department@intechopen.com)

Numbers displayed above are based on latest data collected.  
For more information visit [www.intechopen.com](http://www.intechopen.com)



# Aerodynamic, Structural and Aeroelastic Design of Wind Turbine Blades

*Mohamed Abdou Mahran Kasem*

## Abstract

With the negative impact of conventional energy resources that have been used worldwide, there is a demand for using other resources such as wind energy. Tons of researches have been applied around the globe on the process of designing and manufacturing wind energy conversion systems. In the present chapter, we are concentrating on wind turbine blades' structural design process. The structural design of a wind turbine blade includes defining the wind turbine loads, selecting a suitable material, creating a structural model, and solving the model using the finite element method. This process will be repeated several times until a final design is achieved. The present chapter includes a discussion on the finite element method and wind turbine aeroelasticity.

**Keywords:** wind turbine blades, composite structures, finite element method, aeroelasticity

## 1. Introduction

With the increase in clean energy demand, wind turbine power and subsequently its size increased dramatically. The power generated from wind turbine increased from approximately 30 GW in 2001 to about 600 GW around the globe as depicted in **Figure 1**.

While the total power capacity in Europe increased from about 70 GW to 180 GW in the period from 2008 to 2018, as shown in **Figure 2**, in the United States, the wind power generated from wind turbines increased from 0 to 100 GW in the period from 2000 to 2019 [1].

This increase in wind turbine size makes it important to efficiently design wind turbine structure. A blade structure must be stiff enough, so it does not fail due to wind turbine loads, and at the same moment it should be designed in lightweight and low cost. In the present chapter, we discuss the general structural design process for a wind turbine blade for maximum strength to weight ratio. This process starts by calculating the wind turbine loads, selecting a suitable material, creating a structural model, and applying the finite element method for predicting aeroelastic stability boundaries.

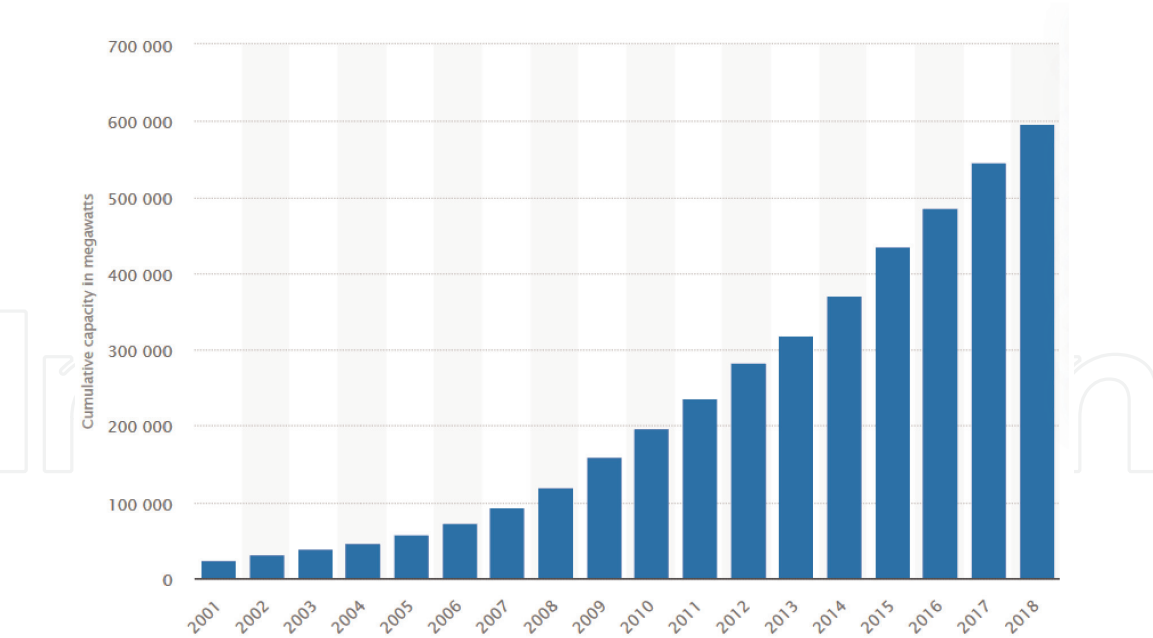


**Figure 1.**  
Global wind power capacity from 2001 to 2018 [1].

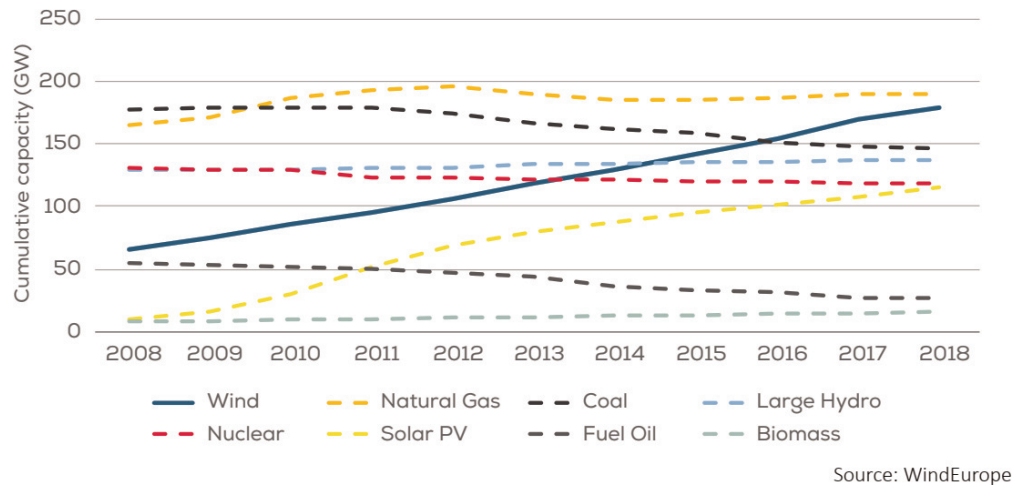


**Figure 2.**  
The European Union's total power generation [2].

## 2. Blade aerodynamic loads

A wind turbine structure must be stiff enough to stand for the flow around. For this reason, the first step in the structure design process is to determine the aerodynamic loads applied to a wind turbine blade. There are mainly two methods for predicting a wind turbine aerodynamic load: blade element momentum (BEM) and computational fluid dynamics (CFD). The BEM can be classified as an analytical method that is fast and accurate. On the other hand, the CFD analysis is a numerical method which is based on numerical and empirical approximations. In general, the BEM is preferred for initial design and load estimation, while the CFD simulation is preferred for detailed design. Designers usually start using BEM in preliminary design and end up using the CFD simulation for detailed analysis and design. A comparison between the BEM and CFD analyses is listed in **Table 1**.

Despite the simplicity of the BEM, it can obtain accurate results as the CFD analysis [3]. However, the BEM is not preferred for detailed simulation. There are software available for both the BEM and CFD analyses, such as wind turbine design

BEM	CFD
Analytical method	Numerical method
Simple to be derived and used	Relatively complex in its formulation and application
Has relatively low computational time	Has relatively high computational time
In general, it does not consider 3D effects (just some corrections such as tip losses)	Depicts 3D effects in detail
Does not consider turbulence effects	Considers turbulence effects
Recommended for preliminary design	Recommended for detailed simulation

**Table 1.**  
*Comparison between the BEM and CFD methods.*

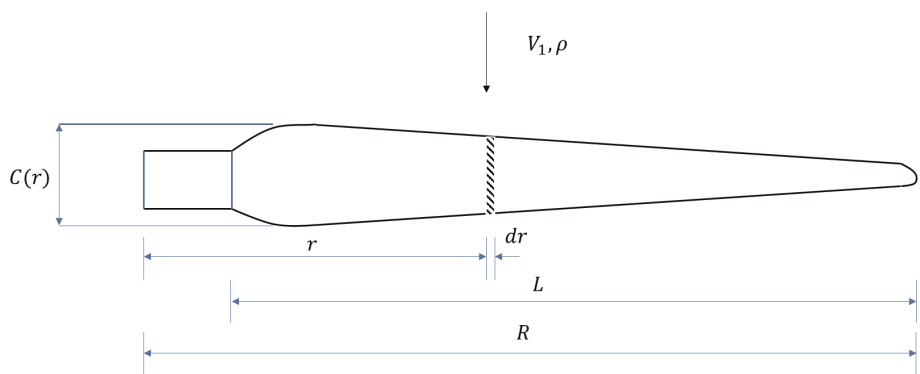


**Figure 3.**  
*BEM model.*

and simulation (Q-blade) that is based on the BEM [4] and ANSYS Fluent that is based on CFD simulation [5]. For more details about ANSYS CFD simulation, we refer the reader to ANSYS Fluent Theory Guide [6]. In the following section, we will summarize the BEM method.

2.1 Blade element momentum theory

The BEM is considered as a simple and fast method in calculating the applied aerodynamic loads on wind turbine blade. The blade is divided into  $N$  radial segments; each segment experiences different chord ( $C$ ), twist angle ( $\beta$ ), and tangential speed ( $\Omega r$ ), as shown in **Figure 3**.

In **Figure 3**,  $V_1$  denotes the upstream velocity,  $\rho$  is the flow density,  $R$  is the rotor radius,  $C$  represents the blade chord, and  $L$  denotes the blade length.  $r$  is the radial position of the rotor section, and  $dr$  defines the blade section width. In the present analyses, we know exactly the blade geometry (chord distribution, angle of twist, and airfoil characteristics), and our objective is to determine the aerodynamic loads applied to the blade (lift and drag).

In BEM, we calculate the forces on each blade element, and then the total forces over the blade can be calculated using summation. The lift force and blade angles are defined in **Figure 4**, which **Figure 4** shows the triangle of in-plane velocity (no subscript), triangle of upstream velocity (subscript 1), and triangle of downstream velocity (subscript 3) [7], where,  $\phi$  is the relative velocity angle.

To simplify the process of calculating blade loads using BEM, we describe it as follows:

1. Start by

$$\phi = \phi_1 = \tan^{-1}\left(\frac{V_1}{\Omega r}\right) = \tan^{-1}\left(\frac{R}{\lambda r}\right) \quad (1)$$

where  $\lambda$  is the tip speed ratio.

2. Set the relative flow speed upper and lower limits:

$$\sin \phi_{max} = \frac{Z \sqrt{1 - \frac{r^2}{R^2}}}{2\pi \frac{r}{R}}, \text{ and } \sin \phi_{min} = \sin\left(\frac{2}{3}\phi_1\right) \quad (2)$$

where  $Z$  represents the number of rotor blades.

3. Calculate the angle of attack from  $\alpha_A = \phi - \beta$ ; then, one can obtain the section lift and drag coefficient from the airfoil characteristics.

4. Calculate the parameter  $x = \sin \phi$ .

If  $x < \sin \phi_{min}$ , use the Glauert correction  
 $\rightarrow x = 0.25 \sin \phi_{min} \sqrt{9 - 2y^2 + 9y^4}$ ,  $y = \frac{\sin \phi}{\sin \phi_{min}}$ , or  
 if  $x > \sin \phi_{max}$ , use the Prandtl correction  $\rightarrow x = \sin \phi_{max}$ .

5. Solve the BEM nonlinear equation to obtain  $\phi$ :

$$\phi = \phi_1 - \tan^{-1}\left(\frac{C_l}{\frac{8\pi r}{Z} x + C_d}\right) \quad (3)$$

6. Repeat steps from 1 to 5 till convergence.

7. After convergence, calculate the relative velocity  $w$ :

$$w = w_1 \cos(\phi_1 - \phi) \frac{\frac{8\pi r}{Z} x}{\frac{8\pi r}{Z} x + C_d} \quad (4)$$

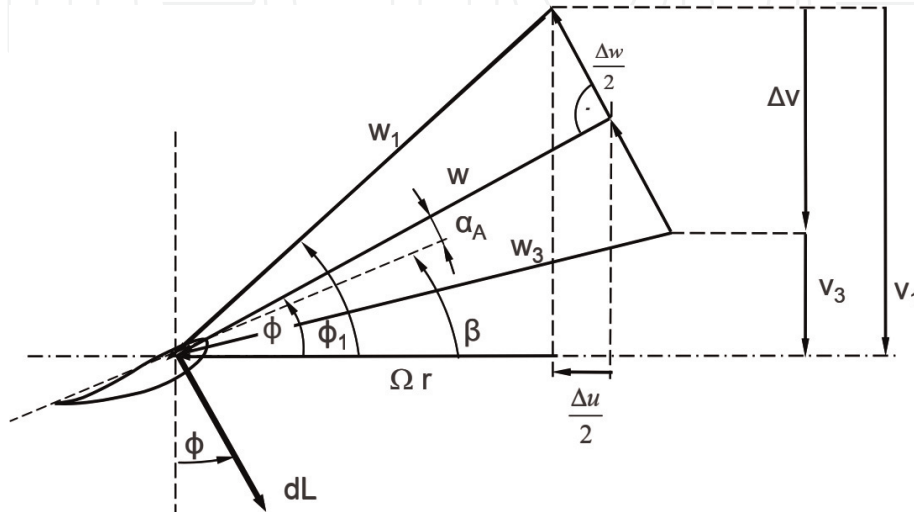


**Figure 4.**  
 Blade element force and angles.

8. Calculate the aerodynamic forces (lift and drag forces):

$$dL = \frac{\rho}{2} w^2 C dr C_l \quad (5)$$

$$dD = \frac{\rho}{2} w^2 C dr C_d \quad (6)$$

- The thrust force can be calculated from the equation:

$$F_n = Z \sum_1^N (dL \cos \phi + dD \sin \phi) \quad (7)$$

where  $N$  represents the number of blade elements.

- The blade tangential (circumferential force)

$$F_z = \sum_1^N (dL \sin \phi - dD \cos \phi) \quad (8)$$

- Blade torque

$$M = \sum_1^N (dL \sin \phi - dD \cos \phi) r \quad (9)$$

Blade power

$$P = \Omega M \quad (10)$$

A schematic for a blade aerodynamic pressure is shown in **Figure 5**. It is seen that the maximum force occurs at the blade root and the minimum at the tip. For this reason, wind turbine blades are usually designed with taper in which the airfoil thickness increases toward the blade root. This property makes the blade structure stiffer at the root and lighter at the tip. For this reason, it is recommended to also design the wind turbine structure with taper. In other words, ribs, spars, and skins have thickness at the blade root higher than the thickness at the tip.

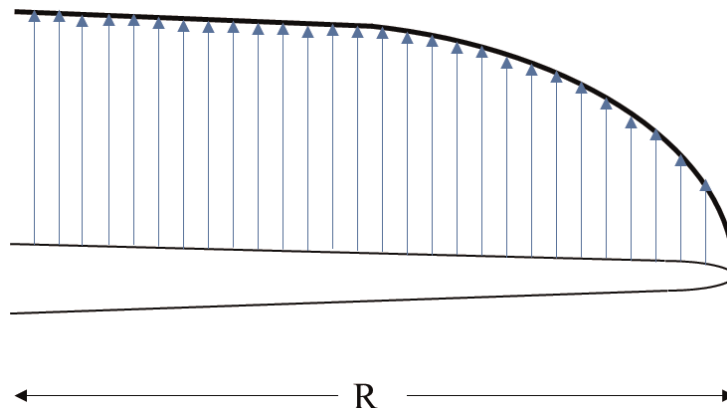


**Figure 5.**  
Schematic for a blade aerodynamic load.



### 3. Material selection

Wind turbines have been made from different materials such as wood, aluminum, and composites. Modern wind turbines are usually made from composites such as carbon fibers and fiber glass. The wide use of composite materials turns to its relative high stiffness to weight ratio in addition to its ability to form complex shapes. Composites are found to be efficient with the large increase in wind turbines' size and capacities. They also can be tailored to satisfy different stiffness and weight requirements. Composite fiber can be used in different orientation to improve the blade directional stiffness in addition to bending and torsional rigidity. **Figure 6** shows the layup process for manufacturing a 6-m-diameter wind turbine that was designed and manufactured at Cairo University laboratories.

Two important things have to be considered when selecting composites: first, selecting the proper fiber direction for a blade structure, and second, insuring that the final product (blade structure) has the same material properties as it was desired in the design process. The former point can be overcome by applying a proper optimization process to select the best laminate configuration for maximizing the blade stiffness to weight ratio, while the latter issue can be resolved by testing the layup configuration after manufacturing some samples to make sure they have the same desired properties plus making experimental tests and measurements to compare between what was designed and what was manufactured.

There are an infinite number of orientations for composite structures. A composite layer can be oriented in any direction. However, it is important when selecting a blade laminate configuration to consider 0, 90, and  $\pm 45^\circ$  angles for the blade skin. These directions are the most important fiber directions to increase the longitudinal, directional, torsional, and bending stiffnesses of a blade (**Figure 7**).

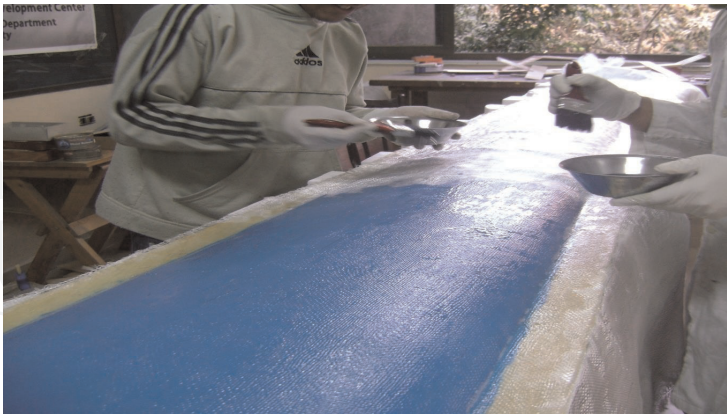


**Figure 6.**  
*Fiberglass/epoxy blade layup.*

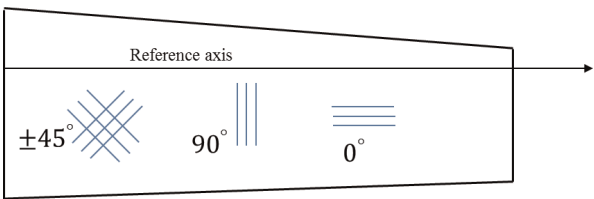


**Figure 7.**  
*Blade skin laminate configuration.*

#### 4. Blade construction and finite element analysis

The objective of wind turbine structure is to transfer and stand for wind turbine loads. Thus, it should be stiff enough to satisfy this objective. The structure weight is also important to be minimum as possible. A typical wind turbine structure consists of the skins, ribs, spar, and root or hub that connects between the blade and the wind turbine tower, as shown in **Figure 8**.

The ribs represent the aerodynamic profile shape for a blade. They distribute the aerodynamic loads and transform them to the main spar, in addition to maintaining the skin profile shape. The skins protect and cover the blade structure elements. Stringers stiffen the skins and connect between the structure of the skins and ribs. A spar represents the main structure element which carries the blade's main loads and transforms them to its root which in turn connects between the blade and the hub. A spar is usually consist of upper and lower flanges (caps) in addition to a shear web (**Figure 9**). The shear web performs high resistance to shear force in which the bending moment over the blade is transformed into in-plane shear forces that are carried by the shear web.

The geometric model available in **Figure 8** represents an equivalent model to the real wind turbine. This model usually is not suitable for finite element (FE) analysis. However, in finite element analysis, we use an equivalent model with some approximations that do not affect the accuracy of the analysis, but these approximations increase the speed and efficiency of the FE process. A geometric model that

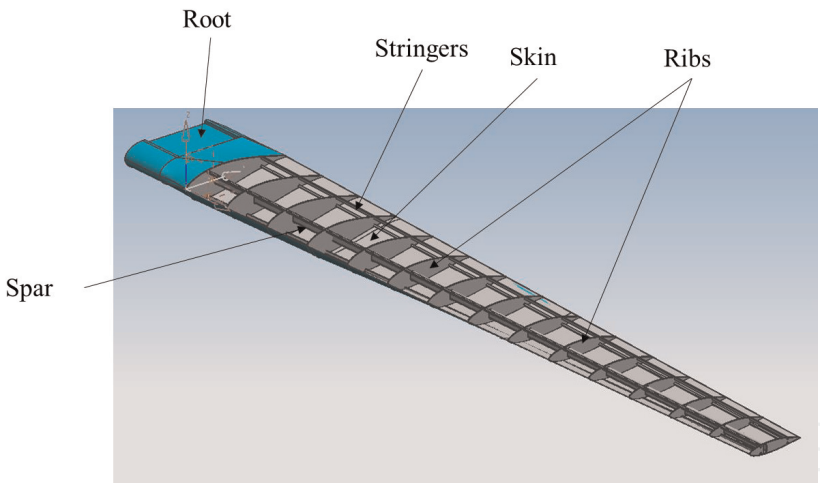


**Figure 8.**  
*A 6-m-diameter typical blade structure.*

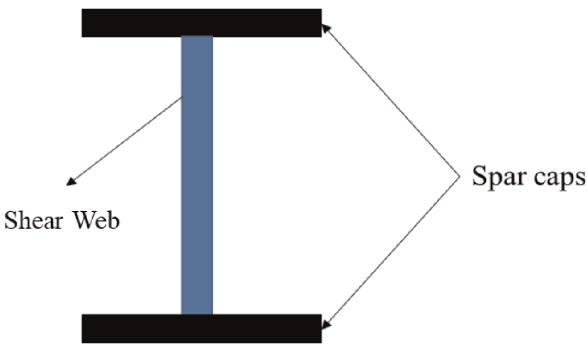


**Figure 9.**  
*A typical blade spar section (I—section).*



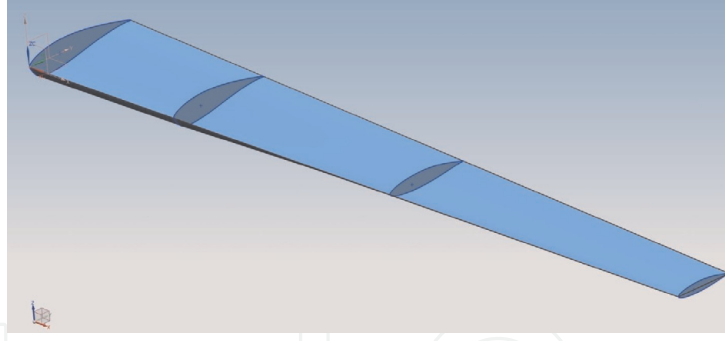


**Figure 10.**  
*Surface approximation for a blade rib and lower skin.*

is physically a 3D model can be approximated into 2D or even 1D simple models. The blade skin and ribs, for instance, have a thickness dimension that is relatively smaller than the other blade dimensions; for this reason the skin and ribs can be approximated into 2D plates in finite element analysis. Geometrically, the blade skin and ribs are modeled as surfaces. Another example is the blade stringers. They have cross-section dimensions that are relatively smaller than the length dimension. Thus, stringers are usually modeled as 1D beams in the finite element analysis. These beams are geometrically represented by lines. These modeling concepts save significant time and effort in structural analysis and design process. An example of a surface approximation for a 6-m-diameter blade ribs and lower skin is shown in **Figure 10**.

In **Figure 10** the blade ribs and skin are represented by surfaces with zero thickness in which we assume there is no change either in stress or strain through their thickness. This approximation is valid as long as the thicknesses of the ribs and skin are relatively smaller than the other surface dimensions. Based on this approximation, a blade is meshed as a 3D model, but it is modeled numerically in FE using quadrilateral element. It is found that higher-order elements such as nine-node element can obtain results more accurate than linear quadrilateral elements in elastic and aeroelastic analyses [8]. So, the element selection is also important. After approximating the blade geometry, selecting the proper element, and defining the finite element model, it is important to perform a convergence test to select the best element size and density for the blade model [9]. **Figure 11** shows how the approximation from the 3D structure model to the 2D reference element is performed and the different reference coordinates that are used.

**Figure 12** shows the geometric model for 10 MW wind turbine blade [11]. The blade has two spars, front and rear spars, in addition to 38 ribs.

The finite element process starts by approximating the physical model as we discussed, then defining the material properties, and selecting a suitable element. After that start the mesh process which transforms the continuous geometric model into discrete elements and nodes. Finally, the model boundary conditions are defined, and the model is solved. The objective of the finite element analysis is to solve the general equilibrium equation [12]

$$\sigma_{ij,j} + f_i = \rho u_{,tt} \quad (11)$$

in which  $\sigma$  is the Cauchy stress tensor,  $\mathbf{f}$  is the force per unit volume, and  $\mathbf{u}$  is the displacement. There are four applicable analyses based on this equilibrium equation:

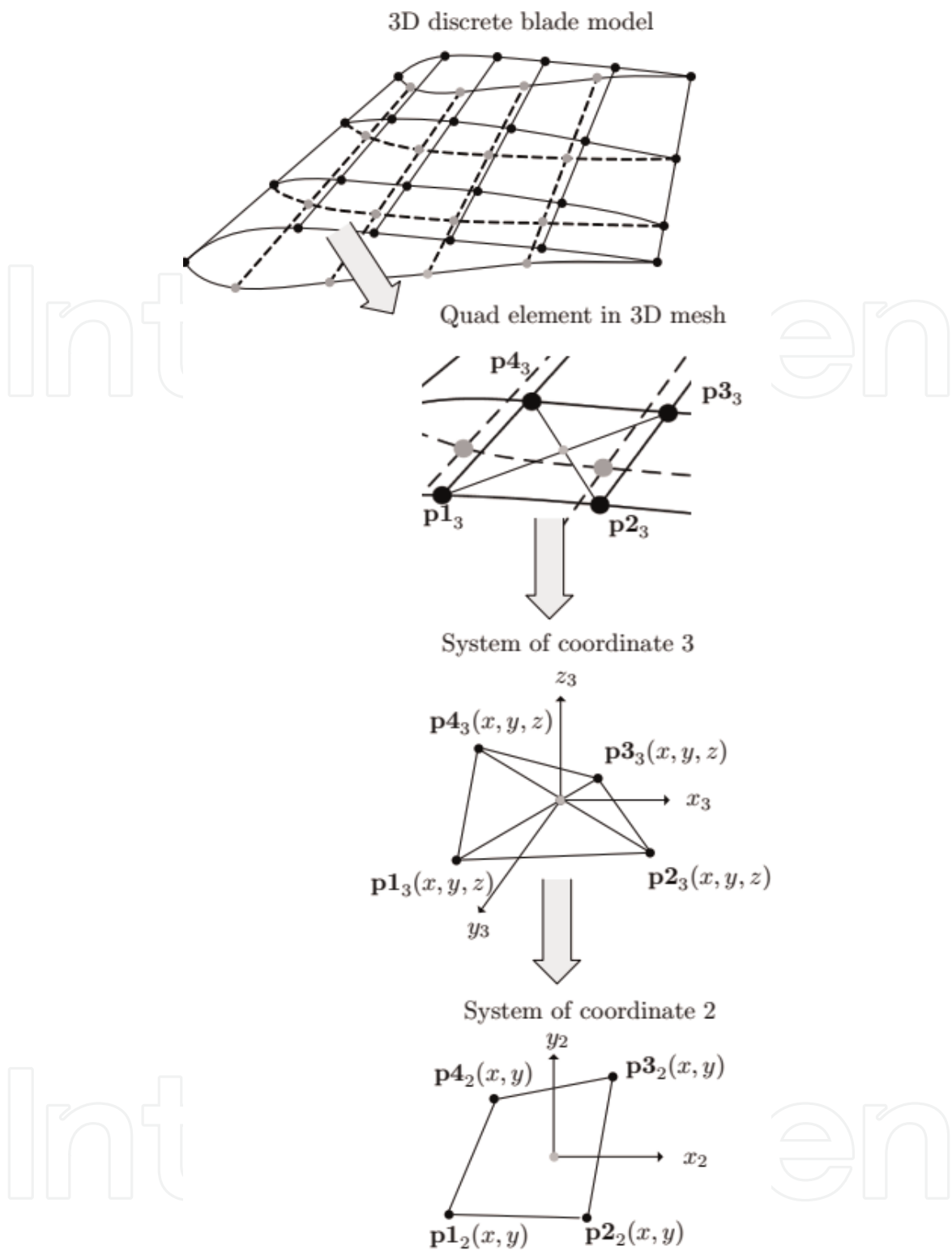


**Figure 11.**  
From a 3D blade finite element mesh to a 2D quadrilateral element [10].

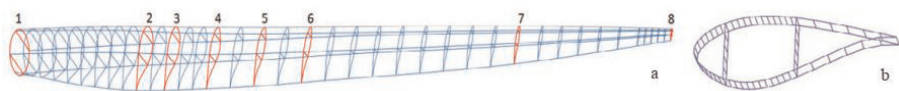


**Figure 12.**  
A 140-m-diameter wind turbine blade geometric model [11].

#### 4.1 Static structural analysis

We called this analysis one-way aeroelastic analysis in which the steady aerodynamic loads are defined and transformed to the structural model and then stresses, strains, and deformations are calculated. It is important in this analysis that the blade maximum deflection satisfy the minimum tower-to-tip clearance [11]. The maximum stresses and strains must be lower than the model allowable stresses and strains. The allowable stresses and strains are defined based on the material yield stresses or strains divided by a factor of safety.

#### 4.2 Modal analysis

In modal analysis, we aim to calculate blade natural modes. Natural modes define the blade natural frequencies and their corresponding mode shapes at which the blade can fail if it excited at any of these modes. Therefore, a blade should be designed with natural frequencies higher than any surrounding frequency.

The modal analysis can be achieved by solving an eigenvalue problem based on the general equilibrium equation that has the form

$$(-\omega^2 \mathbf{M} + \mathbf{K})\mathbf{q} = \mathbf{0} \quad (12)$$

$\mathbf{M}$  and  $\mathbf{K}$  represent the blade mass and stiffness matrices in the finite element model, respectively.  $\mathbf{q}$  represents all the structural nodal degrees of freedom.

#### 4.3 Dynamic analysis

In dynamic analysis, the unsteady aerodynamic loads are transformed into the wind turbine or blade structural model, and then the model is solved considering the time variation of both the loads and structural response. In dynamic analysis, the structure must be stable and safe from failure during its lifetime.

#### 4.4 Aeroelastic analysis

A two-way aeroelastic analysis includes the calculation of blade aerodynamic loads and then transforms these loads into blade structure. After that the structure deformation is calculated and transformed back to the aerodynamic model to calculate new load distribution, and the process goes back and forth until a convergence point is determined. In the following section, we will discuss the wind turbine aeroelastic analysis process.

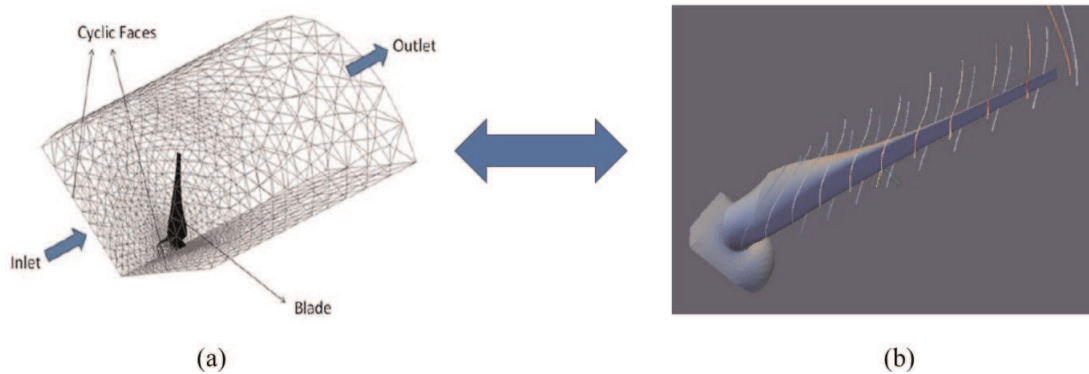


**Figure 13.**

(a) Aerodynamic loads calculated using CFD analysis. (b) The pressure distribution transformed to the blade structure [14].

One of the concerns in aeroelastic analysis is the connection between the aerodynamic model and the structural model. The aerodynamic model is usually made using CFD analysis, while the structural model is usually made using FEM. Different methods have been used to connect between the aerodynamic and structural models such as spline methods that are used in ANSYS software. It is found that the use of the finite element shape functions is more efficient in connecting between the aerodynamic and structural models, than the spline methods [13] (**Figure 13**).

## 5. Aeroelastic analysis of wind turbine blades

With the large increase in wind turbine size, the determination of aeroelastic instability of wind turbine blades becomes a must. Nowadays, wind turbines are designed with high speed, large scale, and light structure. All these specifications make them vulnerable to aeroelastic instabilities. There are two important things in aeroelastic analysis: (1) calculating the exact loads of a wind turbine blade and (2) determining the static (divergence speed) and dynamic (flutter speed) stability limits for a wind turbine.

### 5.1 Aerodynamic loads

In relatively large-scale wind turbines, the structure elastic nature allows it to deform significantly due to the applied aerodynamic loads. This deformation in turn affects the wind turbine thrust and output power. An example is the wind turbine blade shown in **Figure 14**. It is designed for a 1550-kN thrust; however, the wind turbine actual thrust is 1500 due to the aeroelastic effect.

As the wind turbine size becomes larger and larger, these effects become more significant. Therefore, for large-size wind turbines, the aeroelastic effects become more important and can affect significantly the actual wind turbine power. In other words, the wind turbine aeroelastic deformation can significantly decrease the wind turbine power and at the same time decrease the tip-to-tower distance which can lead to wind turbine failure.

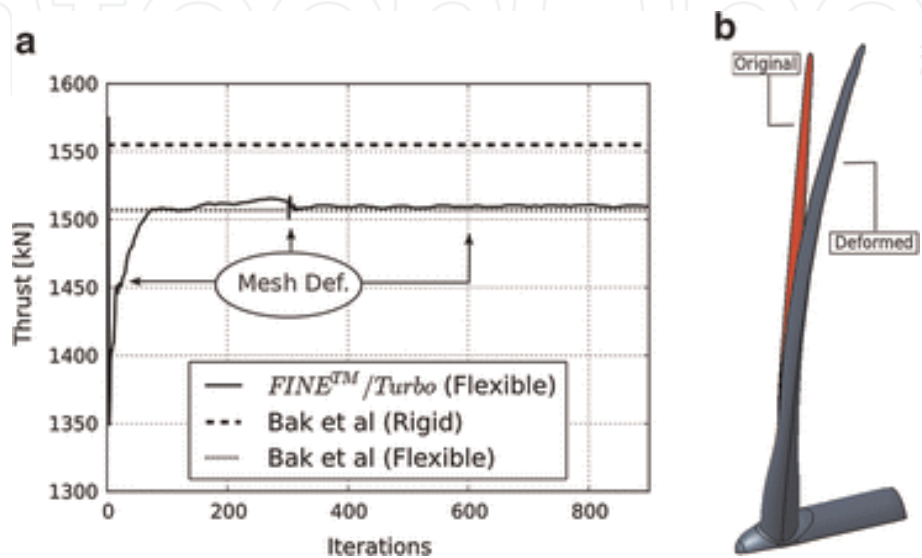


**Figure 14.**  
Aeroelastic effect on the thrust of a 10 MW wind turbine blade [15].

5.2 Static and dynamic aeroelastic instability

The first time for an aeroelastic instability accident to appear was in Washington, USA, in 1940, as a result of Tacoma Narrows Bridge collapse. Then, the aeroelastic instability analyses become important for aerospace structure such as aircraft wings [16] and wind turbines. Recently, researchers start to investigate different aeroelastic phenomena in wind turbines. Aeroelastic instability analysis includes two aeroelastic phenomena: divergence and flutter. The divergence is

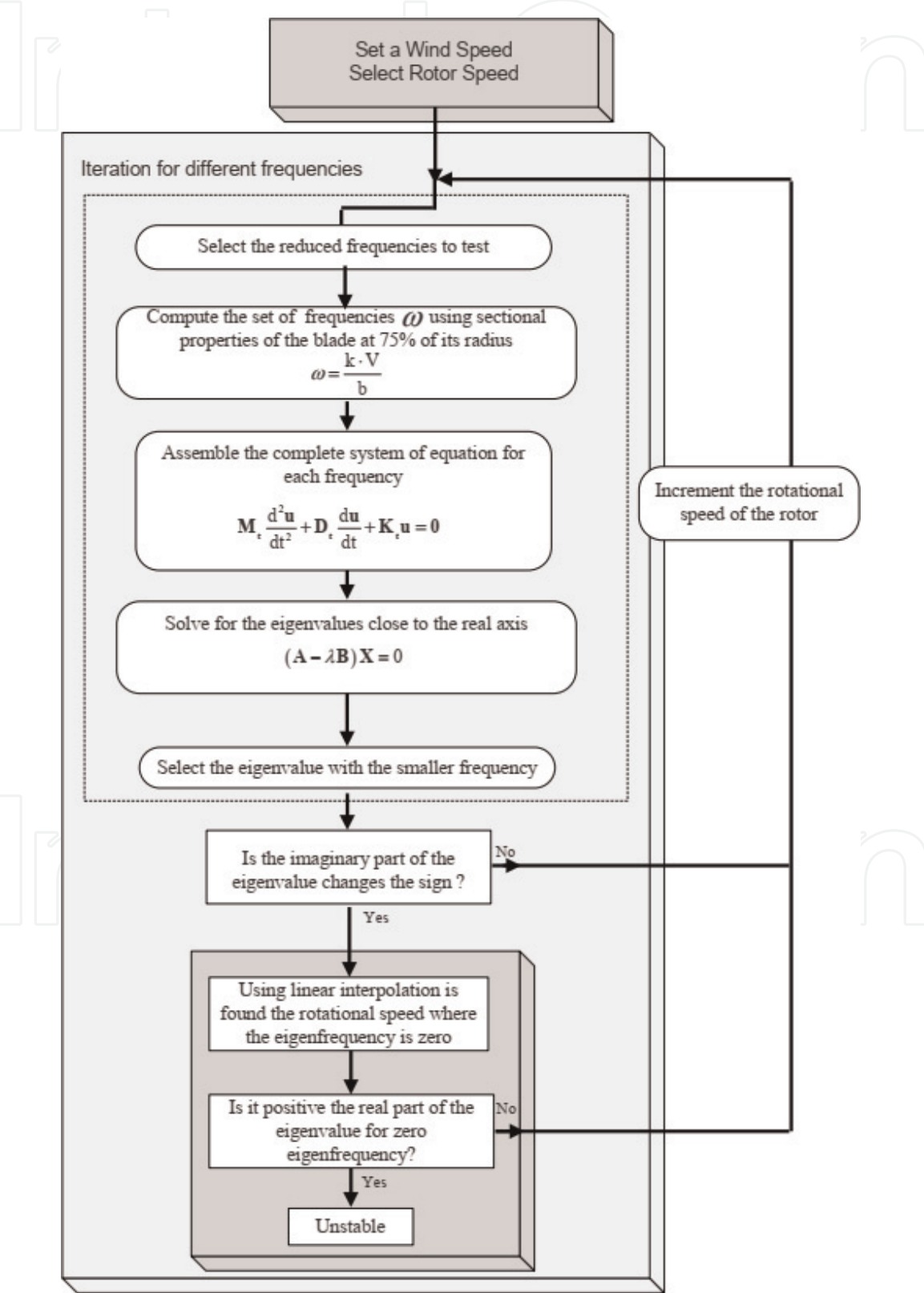
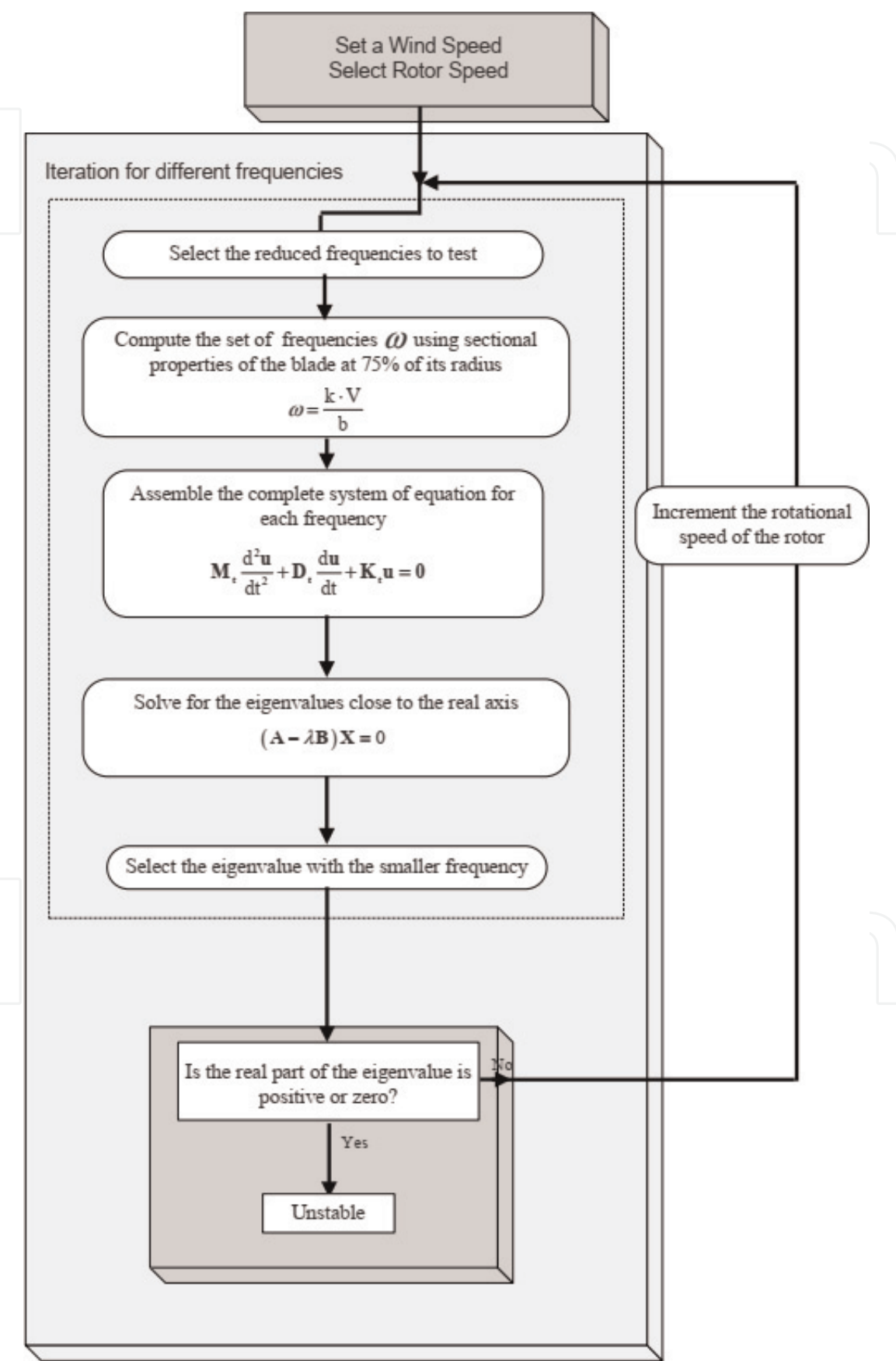


Figure 15.  
A typical iterative process for finding a wind turbine blade divergence speed [10].



known as a static aeroelastic instability due to the blade’s large torsional displacement in response to static aerodynamic loads. It occurs at certain speed known as the divergence speed. On the other hand, flutter is a dynamic aeroelastic instability



**Figure 16.**  
*A typical iterative process for finding a wind turbine blade flutter speed [7].*



that occurs due to unstable vibrations that result from a coupling between twisting and bending modes at certain speed called the flutter speed.

No divergence or flutter failure is recorded for small-scale wind turbines (lower than 10 m diameter) [17] because small wind turbines have relatively stiff structure with low tip speed ratio. In such wind turbines, the flutter speed is found to be five times the wind turbine operating speed [17]. For MW wind turbines, the critical flutter speed becomes lower and lower, and subsequently the aeroelastic analysis becomes more important.

A wind turbine divergence speed is calculated based on steady aerodynamic loads in the interaction with static elastic structure based on an iterative technique. **Figure 15** shows a typical process for determining a wind turbine divergence speed based on the finite element method. On the other hand, a wind turbine flutter speed is calculated based on unsteady aerodynamic loads in the interaction with dynamic elastic structure based on an iterative technique. **Figure 16** shows a typical process for determining a wind turbine flutter speed based on the finite element method.

Notice that the finite element equation given in **Figures 15** and **16**,

$\mathbf{M}_e \frac{d^2 \mathbf{u}}{dt^2} + \mathbf{D}_e \frac{d\mathbf{u}}{dt} + \mathbf{K}_e \mathbf{u} = \mathbf{0}$ , represents the general finite element equation derived from the structure equilibrium equation (Eq. (11)). The first term in the equation represents the structure inertia effects in which  $\mathbf{M}_e$  is the element mass matrix. In divergence analysis the inertia term vanishes, while it is an important and mandatory term in flutter analysis. The second term defines the structure damping effect in which  $\mathbf{D}_e$  is the damping term from both the structure and aerodynamic loads. Then structure damping can only calculate from the experiments. However, if no experiment data available for structure damping, the damping term is defined as a factor multiplied to the structure mass and stiffness matrices. The third term is the structure and aerodynamic stiffnesses. Both the structure and aerodynamic stiffnesses are calculated based on the structure stiffness matrix and the aerodynamic coefficient matrix, respectively. Once, the general finite element equation is defined based on the structure and aerodynamic analyses, it is transformed to an eigenvalue problem to determine the critical speeds for both divergence (**Figure 15**) and flutter (**Figure 16**).


## Author details

Mohamed Abdou Mahran Kasem

Aerospace Engineering Department, Cairo University, Giza, Egypt

\*Address all correspondence to: abdu\_aerospace@eng1.cu.edu.eg

## IntechOpen

© 2020 The Author(s). Licensee IntechOpen. Distributed under the terms of the Creative Commons Attribution - NonCommercial 4.0 License (<https://creativecommons.org/licenses/by-nc/4.0/>), which permits use, distribution and reproduction for non-commercial purposes, provided the original is properly cited. 

## References

- [1] Wind Energy Facts at a Glance | AWEA [Online]. Available from: <https://www.awea.org/wind-101/basics-of-wind-energy/wind-facts-at-a-glance> [Accessed: 15 September 2019]
- [2] WindEurope—The Voice of the Wind Energy Industry. WindEurope [Online]. Available from: <https://windeurope.org/> [Accessed: 15 September 2019]
- [3] Bangga G. Comparison of blade element method and CFD simulations of a 10 MW wind turbine. *Fluids*. 2018; **3**(4):73
- [4] QBlade [Online]. Available from: <http://www.q-blade.org/> [Accessed: 22 March 2017]
- [5] Simulation Driven Product Development | ANSYS [Online]. Available from: <http://www.ansys.com/> [Accessed: 07 February 2017]
- [6] Ahmad T, Plee SL, Myers JP. FLUENT Theory Guide. ANSYS; 2011. p. 826. Available from: [https://www.afs.enea.it/project/neptunius/docs/fluent/html/th/main\\_pre.htm](https://www.afs.enea.it/project/neptunius/docs/fluent/html/th/main_pre.htm)
- [7] Gasch R, Tvele J, editors. *Wind Power Plants*. Berlin/Heidelberg: Springer; 2012
- [8] Mahran M, Elsabbagh A, Negm H. A comparison between different finite elements for elastic and aero-elastic analyses. *Journal of Advanced Research*. 2017; **8**(6):635-648
- [9] Mahran M, Negm H, Elsabbagh A. *Aeroelastic Analysis of Plate Wings Using the Finite Element Method*. Lab Lambert Academic Publishing; 2015. Available from: <https://www.lap-publishing.com/catalog/details/store/gb/book/978-3-659-67969-8/aero-elastic-analysis-of-plate-wings-using-the-finite-element-method?locale=gb>
- [10] Capponi P. A finite element approach for aeroelastic instability prediction of wind turbines [Master]. [Thesis]. Delft, Netherlands: TU Delft; 2010
- [11] Cox K, Echtermeyer A. Structural design and analysis of a 10MW wind turbine blade. *Energy Procedia*. 2012; **24**: 194-201
- [12] Kasem MM, Dowell EH. A study of the natural modes of vibration and aeroelastic stability of a plate with a piezoelectric material. *Smart Materials and Structures*. 2018; **27**(7):075043
- [13] Mahran M, Negm H, El-Sabbagh A. Aero-elastic characteristics of tapered plate wings. *Finite Elements in Analysis and Design*. 2015; **94**(Supplement C): 24-32
- [14] Elqatary IHS. *Experimental Characterization for Variable Pitch Horizontal Axis Wind Turbine*. [Thesis]. Egypt: Cairo University; 2013
- [15] Horcas SG, Debrabandere F, Tartinvill B, Hirsch C, Coussement G. Hybrid mesh deformation tool for offshore wind turbines aeroelasticity prediction. In: *CFD for Wind and Tidal Offshore Turbines*. Cham: Springer; 2015. pp. 83-94
- [16] Kasem MM, Negm H, El-Sabbagh A. Aeroelastic modeling of smart composite wings using geometric stiffness. *Journal of Aerospace Engineering*. 2019; **32**(2):04018143
- [17] Vatne SR. *Aeroelastic instability and flutter for a 10 MW wind turbine* [Master]. [Thesis]. Trondheim: Norwegian University of Science and Technology; 2011